Bioorganic & Medicinal Chemistry 20 (2012) 6523–6532

Contents lists available at SciVerse ScienceDirect

Bioorganic & Medicinal Chemistry

journal homepage: www.elsevier.com/locate/bmc

Synthesis of a potent photoreactive acidic γ-secretase modulator for target identification in cells

Andreas Rennhack [a], Thorsten Jumpertz [b], Julia Ness [b], Sandra Baches [b], Claus U. Pietrzik [c], Sascha Weggen [b,*], Bruno Bulic [a,*]

[a] Research Group Chemical Biology of Neurodegenerative Diseases, Center of Advanced European Studies and Research, Ludwig-Erhard-Allee 2, D-53175 Bonn, Germany
[b] Department of Neuropathology, Heinrich-Heine-University, D-40225 Duesseldorf, Germany
[c] Molecular Neurodegeneration Group, Institute of Pathobiochemistry, University Medical Center of the Johannes Gutenberg-University, D-55099 Mainz, Germany

ARTICLE INFO

Article history:
Received 30 May 2012
Revised 23 July 2012
Accepted 8 August 2012
Available online 31 August 2012

Keywords:
Alzheimer's disease
Proteases
Secretase inhibitors
Secretase modulators
Photoreactive probes
Diazirine
Target identification
Drug development

ABSTRACT

Supramolecular self-assembly of amyloidogenic peptides is closely associated with numerous pathological conditions. For instance, Alzheimer's disease (AD) is characterized by abundant amyloid plaques originating from the proteolytic cleavage of the amyloid precursor protein (APP) by β- and γ-secretases. Compounds named γ-secretase modulators (GSMs) can shift the substrate cleavage specificity of γ-secretase toward the production of non-amyloidogenic, shorter Aβ fragments. Herein, we describe the synthesis of highly potent acidic GSMs, equipped with a photoreactive diazirine moiety for photoaffinity labeling. The probes labeled the N-terminal fragment of presenilin (the catalytic subunit of γ-secretase), supporting a mode of action involving binding to γ-secretase. This fundamental step toward the elucidation of the molecular mechanism governing the GSM-induced shift in γ-secretase proteolytic specificity should pave the way for the development of improved drugs against AD.

1. Introduction

Over the last decade, regulated proteolysis has emerged as an important cellular activity involved in various biological processes such as cell differentiation, stress response or transcriptional regulation. Two percent of the human genome encodes for proteolytic enzymes, and deregulations of the 'degradome' have been linked to various disorders, such as haemophilia, obesity and cancer.[1,2] Notably, the familial hereditary form of Alzheimer's disease (FAD), which accounts for ca. 1–2% of cases of Alzheimer's disease (AD), is associated with mutations in the genes encoding for presenilins, the catalytic subunits of γ-secretase and the amyloid precursor protein (APP).[3–5]

AD is a progressive neurodegenerative disorder characterized by the presence of intracellular neurofibrillary tangles and extracellular amyloid plaques in the cerebral cortex and hippocampus.[6–8] Amyloid plaques are essentially formed by the self-assembly of the 42 amino acids-long Aβ42 peptides, produced by cleavage of APP at synaptic terminals by aspartyl proteases (Fig. 1).[9,10] After shedding of the extracellular domain of APP by the β-secretase, the membrane-bound C99 fragment is subsequently processed within its transmembrane domain by the γ-secretase complex. Interestingly, the substrate is not cleaved at a single position; heterogeneous fragments are secreted and range in lengths from 37 to 43 amino acids.[11,12] Investigations of the proteolytic mechanism providing a predominantly 40 amino acids-long peptide are complicated by the multimeric nature of the γ-secretase complex which includes, besides the presenilins 1 or 2 (PS1/2) N- and C-terminal fragments forming the catalytic core, multiple accessory proteins (APH-1, nicastrin, PEN-2).[13,14] While the impact of the Aβ42 peptide on cell viability has been extensively investigated in vitro and in vivo, the physiological role of the γ-secretase and its multiple other substrates remains unclear.[9,10] Altogether, avoiding the formation of amyloid plaques remains a promising therapeutic approach for FAD and, plausibly, for sporadic AD.[15,16] Unfortunately, previous clinical trials operating on full inhibition of γ-secretase with the objective to 'trim down' the production of

Abbreviations: Aβ, amyloid-β peptide; GSM, γ-secretase modulator; GSI, γ-secretase inhibitor; APP, amyloid precursor protein; PS1/2, presenilin 1/2; PS1-NTF, N-terminal fragment of PS1; AD, Alzheimer's disease; FAD, familial Alzheimer's disease; APH-1, anterior pharynx defective-1; PEN-2, presenilin enhancer-2; NCT, nicastrin; NSAID, non-steroidal anti-inflammatory drug.

* Corresponding author. Tel.: +49 228 9656401.
E-mail address: bruno.bulic@caesar.de (B. Bulic).

0968-0896/$ - see front matter © 2012 Elsevier Ltd. All rights reserved.
http://dx.doi.org/10.1016/j.bmc.2012.08.034

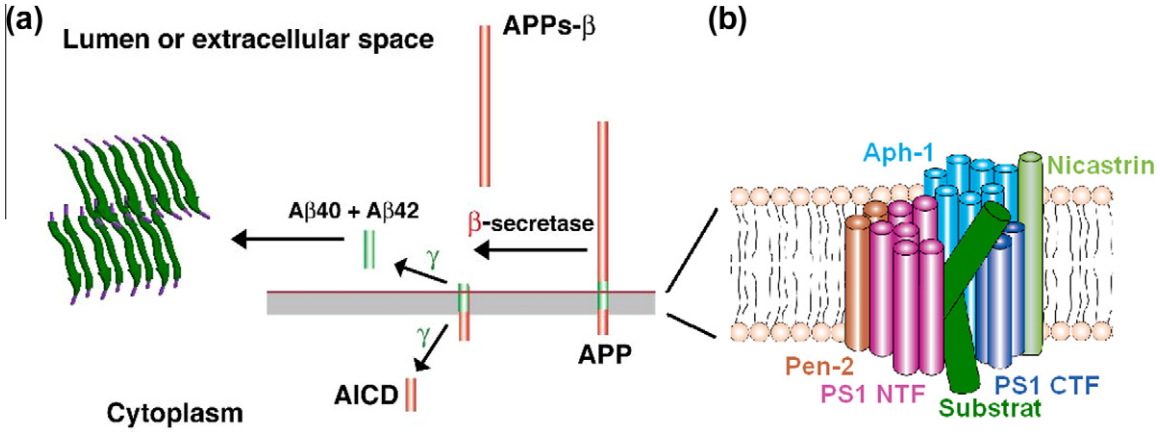

Figure 1. Schematic representations of (a) sequential cleavage of APP substrate by β- and γ-secretases leading to the formation of Aβ40 and Aβ42 peptides. (b) γ-Secretase complex with PS1-NTF (purple), APH-1 (blue), nicastrin (light green), PEN-2 (orange) and a substrate molecule (dark green).

the culprit amyloidogenic Aβ42 peptides failed due to severe side effects likely linked to broad inhibition of the constitutive functions of γ-secretase. Interestingly, compounds termed γ-secretase modulators (GSMs) preserve the constitutive activity of γ-secretase and only shift the cleavage specificity toward less amyloidogenic fragments such as Aβ38.[17] Clearly, unlike the quantitative effect of γ-secretase inhibitors, the qualitative action of GSMs may allow the protease to keep on performing its physiological functions.

Since the early identification of GSMs in the class of non-steroidal anti-inflammatory drugs (NSAIDs), intensive efforts in medicinal chemistry to improve their low blood–brain barrier permeability and moderate potency have yielded second-generation GSMs in two distinct classes (acidic and non-acidic GSMs), named after a characteristic carboxylic acid.[18–21] However, their molecular mechanism of action remains largely unknown. Strong evidence gained from in vitro investigations with partially purified protease support a direct action of the compounds on the γ-secretase complex itself.[22–24] Furthermore, cross-competition binding assays between radiolabeled inhibitors and NSAID GSMs indicated that transition-state inhibitors were displaced in a non-competitive manner, suggesting different binding sites and an allosteric mode of action for GSMs.[22,25] Moreover, fluorescence lifetime imaging has been used to monitor conformational changes at the PS1 epitope of γ-secretase, indicating a closure of a hydrolytic site upon incubation with GSMs.[26,27] In contrast to these findings, several research teams reported the binding of NSAID GSMs to the APP substrate rather than to the γ-secretase.[28–30] However, the very low potencies and specificities of the used GSMs prompted further investigations questioning the validity of the proposed APP binding, with strong evidence for self-aggregation and promiscuous binding.[31–33]

We therefore embarked on the synthesis of diazirine-modified probes for photoaffinity labeling based on the highly potent second-generation acidic modulator **GSM-1** (Fig. 2). The design criteria included: low steric bulk, high potency, stability of the photoreactive moiety and photolysis wavelength compatible with experiments in live cells. After optimization of a diazirine-compatible synthetic route and elucidation of a preliminary structure–activity relationship for the **GSM-1** scaffold, we could successfully synthesize the **AR243** probe equipped with a photoreactive diazirine moiety and a biotin tag for affinity purification, along with a nanomolar modulatory activity and high structural fidelity to the parent compound (Fig. 2). However, the biotin tag, with its relative high polarity and steric bulk, required the incorporation of an adequate spacer and, in this respect, copper-catalyzed click chemistry presents an attractive alternative.[34] Nonetheless, photolabeling experiments

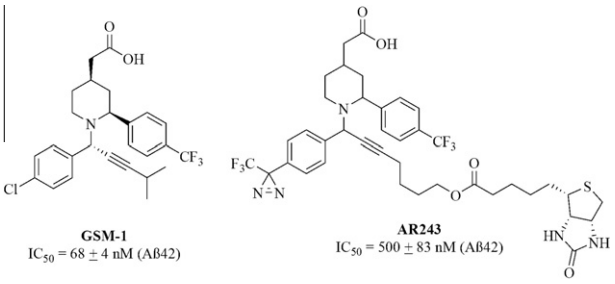

Figure 2. Left: Parent acidic phenylpiperidine-type GSM **GSM-1**. Right: Derived photoprobe **AR243** with photoreactive diazirine moiety and biotin-tag for affinity purification.

using our biotinylated probe provided evidence for direct binding to the γ-secretase complex at the PS1-NTF epitope.[35] This is consistent with recent data obtained from investigations in the class of imidazole-based non-acidic GSMs showing binding to Pen2 and PS1-NTF.[36,37] Moreover, comparable photoaffinity labeling studies with benzophenone- and azide-equipped acidic modulators, but no diazirine-GSM, appeared in the recent literature.[34,38]

The 3-phenyl-3-(trifluoromethyl)-3*H*-diazirine (in the following referred to as diazirine) photoreactive group was primary selected for its interesting characteristics. That is low steric bulk, high lipophilicity and long wavelength of activation (~350 nm). Diazirines have been successfully used as photolabeling reagents since their first synthesis by Brunner et al. in 1980 and their application has been reviewed extensively.[39–43] We hereafter describe the design and synthesis of **GSM-1** derived, diazirine-equipped photoreactive probes as well as a preliminary structure–activity relationship around this compound class.

2. Results

2.1. Chemistry

2.1.1. Diazirine-compatible Cu(I)-catalyzed A^3-coupling

The synthesis of the parent modulator **GSM-1** is described in the patent literature and involves the reaction of α-phenyl amines with benzaldehydes under Dean–Stark conditions prior to the addition of an organozinc reagent.[44] However, the route proved impractical for diazirine-modified **GSM-1** derivatives because the diazirine group appeared thermally labile. We therefore investigated metal-catalyzed three-component coupling reactions with copper, iron,

indium or gold replacing the organozinc reagent with a terminal alkyne to widen the substrate scope and to provide milder reaction conditions (A^3-coupling, Scheme 1).[45–48] From these catalysts only copper(I) appeared to be suitable for our diazirine-based approach and after several optimization rounds, we could obtain the desired coupling products in satisfactory yield. In the successful setup three equivalents of copper(I)-bromide with respect to the aldehyde were used and the reactions were run at 90 °C for 24 h in toluene with a 2:1:1 stoichiometry with respect to amine, aldehyde and alkyne in the presence of activated 4 Å-molecular sieves (General method A; see Section 5). Lowering the reaction temperature to 60 °C and increasing the reaction time to 48 h could further prevent thermal decomposition of the diazirine and was therefore chosen for the synthesis of photoreactive derivatives (General method B; see Section 5). Increasing the stoichiometry of alkynes and amines provided only minor improvement. The products of the three-component couplings were subsequently purified and submitted to further manipulations on side chains to provide the final compounds (as described below and in the Supplementary data).

2.1.2. Synthesis of building blocks

Amine **1** was obtained according to the patent literature in racemic and enantiomeric pure forms, and served as a starting material for the silyl-protected analog **5**, which was synthesized via the intermediates **2** and **3** (Scheme 2A).[44] Esterification of **3** with 2-trimethylsilylethanol and subsequent hydrogenolytic N-debenzylation of the intermediate **4** yielded the desired protected ester **5**. Orthogonal protection of the piperidine-bound carboxylic acid was necessary as we planned to link the biotin tag via an ester bond for reasons of higher lipophilicity compared to the more common primary amide-link (see also Section 3.1 and Scheme 1). Required terminal alkynes were synthesized from commercial 5-hexyn-1-ol by acylation with biotin or acetic anhydride,[49] yielding esters **6** and **7** (Scheme 2B), respectively. Amino-alkyne **9** was obtained via the free amine **8** starting from commercial *N*-(5-hexynyl)phthalimide by treatment with hydrazine hydrate and reprotection using Boc-anhydride (Scheme 2B). Non-commercial benzaldehydes were synthesized as outlined in Scheme 3. Briefly, 3-methoxy-4-(4-methyl-1*H*-imidazol-1-yl)benzaldehyde **10** was obtained as described in the patent literature from 4-(5)-methylimidazole and 4-fluoro-3-methoxy-benzaldehyde.[50] Following the protocol from Chen et al.,[51] we obtained the diazirine-equipped benzaldehyde **14** starting from commercial 1,4-dibromobenzene (Scheme 2). The so obtained intermediate 4-trifluoroacetylbenzoic acid **11** was esterified with methanol to **12**, followed by oxime formation and tosylation to provide **13**. Subsequently, treatment with liquid ammonia in DCM afforded the corresponding intermediate diaziridine. The sensitive oxidation to obtain the diazirine was finally accomplished under Swern conditions.[52] Reduction of the methylester to the aldehyde using DIBAL or milder reducing agents such as SDBBA unfortunately resulted in decomposition of the diazirine.[53] However, its precursor, the trifluoromethyl diaziridine-methyl benzoate, was found to be stable toward SDBBA-mediated reduction. Therefore, undertaking the reduction step before the diaziridine-oxidation, we could obtain the aldehyde **14** with a 40% overall yield.

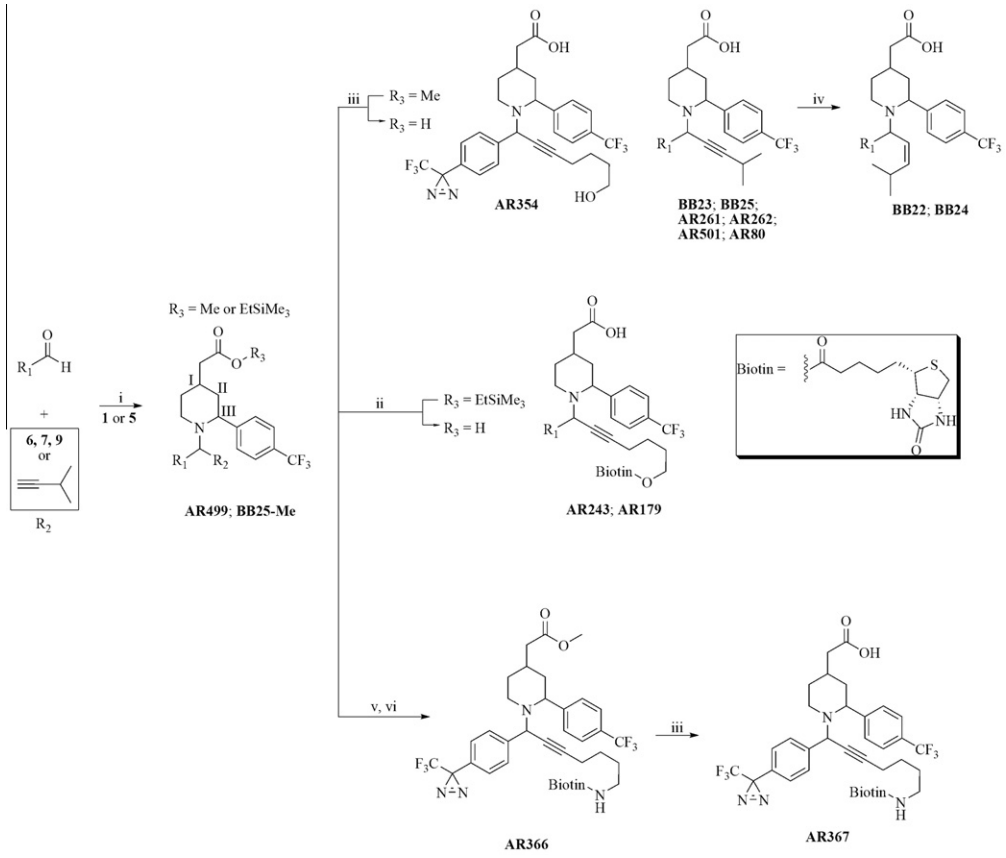

Scheme 1. Synthesis of phenylpiperidine-type GSMs via A^3-coupling and subsequent side chain modifications. R_1–R_3 as well as numbering of stereocenters refer to Table 1. Reagents and conditions: (i) CuBr, activated 4 Å-mol sieves, PhMe, 90 °C, 24 h or 60 °C, 48 h; (ii) TBAF, THF, rt, 2 h; (iii) LiOH–H_2O, THF/H_2O/MeOH, rt, 2 h; (iv) Lindlar's cat, quinoline, H_2, 1 atm, PhMe, rt, 7 h; (v) 4 M HCl, dioxane, rt, 2 h; (vi) biotin, EDAC, DIPEA, DMF, rt, 2 h (for detailed synthetic procedures and spectroscopic data the reader is referred to the Supplementary data).

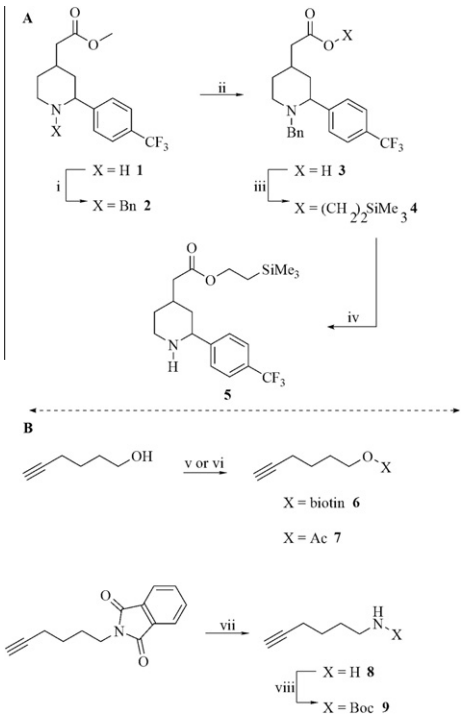

Scheme 2. (A) Synthesis of silyl-protected amine **5**. Reagents and conditions: (i) BnBr, KI, CH_3CN, rt, 15 min; (ii) $LiOH{\cdot}H_2O$, $THF/H_2O/MeOH$, rt, 2 h;[44] (iii) $HO(CH_2)_2SiMe_3$, EDAC, DMAP, DCM, rt, 3 h; (iv) Pd/C, H_2 1 atm, ^{i}PrOH, rt, 24 h. (B) Synthesis of terminal alkynes **6**, **7** and **9**: (v) biotin, TBTU, DIPEA, DMF, rt, 5 h; (vi) Ac_2O, Py/DCM, rt, 3 h;[49] (vii) $(H_2N)_2$-H_2O, THF, reflux, 3 h; (viii) Boc_2O, $NaHCO_3$, THF/H_2O, rt, 2 h (for detailed synthetic procedures and spectroscopic data the reader is referred to the Supplementary data).

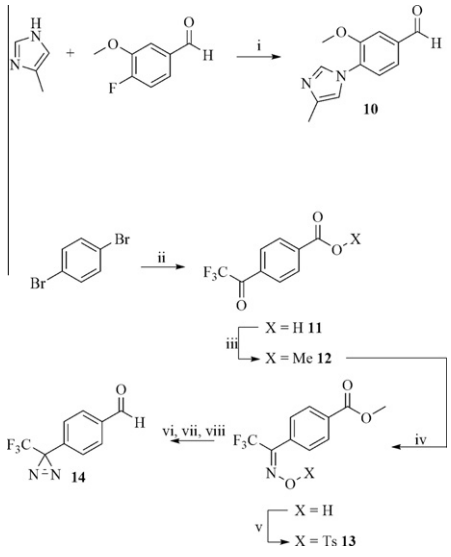

Scheme 3. Synthesis of **10** and diazirine-tagged benzaldehyde **14**. Reagents and conditions: (i) K_2CO_3, DMF, 50 °C, over night;[50] (ii) 1. *n*-BuLi, CF_3COOMe, THF, −78 °C, 1 h/2. *n*-BuLi, CO_2 (s), THF, −78 °C to rt, 2 h;[51] (iii) H_2SO_4, MeOH, 60 °C, over night; (iv) $H_2NOH{\cdot}HCl$, MeOH/Py, reflux, over night; (v) TsCl, NEt_3, DCM, 0 °C to rt, 1 h; (vi) NH_3 (l), DCM, −78 °C to rt, over night; (vii) SDBBA, THF, 0 °C, 40 min;[53] (viii) $(COCl)_2$, DMSO, NEt_3, DCM, −78 °C to rt, 1 h.[52]

2.1.3. GSM synthesis and structure–activity relationship

With the optimized protocol for the copper(I)-catalyzed A^3-coupling and building blocks in hand, we were able to synthesize a subset of 15 structurally divergent GSMs including the desired photoprobes (Scheme 1 and Table 1). In addition we were able to establish a preliminary structure–activity relationship for straight and inverse GSMs.

By reacting the enantiomeric pure forms of amine **1** with 4-chlorobenzaldehyde and 3-methylbut-1-yne followed by ester hydrolysis, we could obtain the enantiomers **BB25** and **BB23**, which minimally differed from the parent **GSM-1** structure by an internal alkyne required for this milder synthesis route (Scheme 1 and Table 1). CHO cells stably overexpressing wild-type APP and PS1 were incubated with the compounds to determine their potency against Aß42 and selectivities versus Aß40 (all) and Aß38 (only for selected compounds) (Table 1 and Supplementary Figs. S1(A–F) and S2) by sandwich ELISA of cell-culture supernatants.[3] The ELISA data for **BB25** and **BB23** revealed that the alkyne introduction was well tolerated, as reflected by activities comparable to the parent modulator **GSM-1** (IC_{50} = 68 ± 4 nM (Aβ42) Table 1, entry 1; **BB25**: IC_{50} = 87 ± 8 nM (Aβ42); **BB23**: IC_{50} = 300 ± 0 nM (Aβ42); entries 2 and 3). In addition, **BB25** showed the typical profile of an acidic GSM, selectively lowering Aß42 while raising Aß38 and having no significant impact on Aß40 levels (Supplementary Figs. S1A, B and S2). Each enantiomer displayed a distinct potency, as often observed for drugs targeting chiral domains within biomolecules. As reported for NSAID-like acidic GSMs, esterification of the characteristic carboxylic acid of **BB25** to give **BB25-Me** reversed the activity profile of the compound, turning the modulation from selective Aβ42 lowering (IC_{50}) to Aβ42 elevating (EC_{50}), in a yet incompletely understood manner (**BB25-Me**: EC_{50} = 2.5 ± 0.3 μM (Aβ42); entry 4 and Supplementary Fig. S2). [19,54]

In an effort to come closer to the parent **GSM-1** structure, hydrogenation of the alkyne in **BB23** and **BB25** was probed under various conditions, ending unfortunately in decomposition through dehalogenation. However, we were able to isolate **BB22** and **BB24** after partial hydrogenation using Lindlar's catalyst (Scheme 1), bearing a *cis*-alkene in its side-chain. Interestingly, the potency of the more active enantiomer **BB24** (IC_{50} = 30 ± 1 nM (Aβ42); entry 5 and Supplementary Fig. S2) improved over the parent compound **BB25** whereas the potency of the opposite enantiomer **BB22** further decreased (IC_{50} = 616 ± 12 nM (Aβ42); entry 6 and Supplementary Fig. S2). However, due to only moderate gain in potency and restricted compatibility of hydrogenation reactions with diazirines, we selected **BB25** for further probe-development as detailed below.

We next investigated the structure–activity relationship around the lower chloro-aryl moiety as a potential introduction site for the photoreactive diazirine. By substituting 4-chlorobenzaldehyde with 3-methoxy-4-(4-methyl-1*H*-imidazol-1-yl)benzaldehyde **10** we obtained **AR501**, which shares the characteristic imidazole commonly observed in the class of non-acidic GSMs (Scheme 1 and Table 1).[19,50] However, the disappointing activity for **AR501** (IC_{50} = 1.0 ± 0.1 μM (Aβ42); entry 7 and Supplementary Fig. S2) indicated sensitivity to polarity effects at this site. Interestingly, the corresponding inverse modulator **AR499** (EC_{50} = 1.6 ± 0.2 μM (Aβ42); entry 8 and Supplementary Fig. S2), the methylester analogue of **AR501**, presented a comparable activity to **BB25-Me** (2.5 ± 0.3 μM) in raising Aß42, while the potencies of the respective straight modulators **BB25** and **AR501** differed significantly (IC_{50} = 87 ± 8 nM vs 1.0 ± 0.1 μM, respectively), underlining the apparent disconnect in SAR between straight and inverse modulators. To further determine the sensitivity of the site toward polarity effects, we substituted the chlorine for a trifluoromethyl group using commercial 4-trifluoromethyl benzaldehyde (Scheme 1 and Table 1). The resulting enantiomers **AR262** (IC_{50} = 50 ± 4 nM (Aβ42); entry 9 and Supplementary Fig. S2) and **AR261** (IC_{50} = 350 ± 35 nM (Aβ42); entry 10 and Supplementary Fig. S2) displayed similar potency as their chlorine analogs **BB25** and **BB23** (87 ± 8 nM and 300 ± 0 nM, respectively), emphasizing the tolerance of lipophilicity in this

Table 1
Structures and activities of acidic phenylpiperidine GSMs

Entry	Compound	Stereo-chemistry[a]	R_1[b]	R_2[b]	R_3[b]	IC_{50}/EC_{50} ± SEM (Aß42)[c]
1	**GSM-1**	I: S II: R III: S	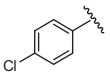		H	68 ± 4 nM
2	**BB25**	I: S II: R III: S	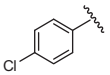		H	87 ± 8 nM
3	**BB23**	I: R II: S III: R	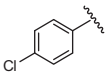		H	300 ± 0 nM
4	**BB25-Me**	I: S II: R III: S	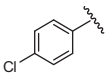		Me	Inverse 2.5 ± 0.3 μM
5	**BB24**	I: S II: R III: S	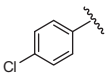		H	30 ± 1 nM
6	**BB22**	I: R II: S III: R	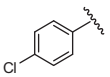		H	616 ± 12 nM
7	**AR501**	rac	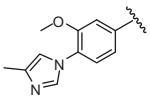		H	1.0 ± 0.1 μM
8	**AR499**	rac	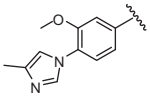		Me	Inverse 1.6 ± 0.2 μM
9	**AR262**	I: S II: R III: S	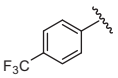		H	50 ± 4 nM
10	**AR261**	I: R II: S III: R	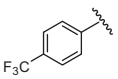		H	350 ± 35 nM
11	**AR80**	rac	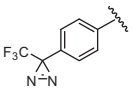		H	190 ± 14 nM
12	**AR179**	rac	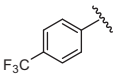	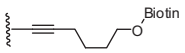	H	1.0 ± 0.0 μM
13	**AR243**	rac	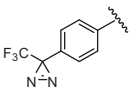	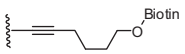	H	500 ± 83 nM
14	**AR366**	rac	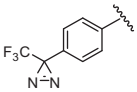	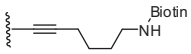	Me	Inverse 1.1 ± 0.1 μM
15	**AR367**	rac	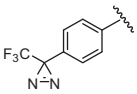	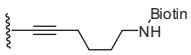	H	2.2 ± 0.1 μM
16	**AR354**	rac	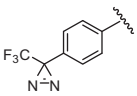	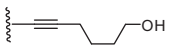	H	2.0 ± 0.1 μM

For dose response curves and selectivity data of selected compounds the reader is referred to the Supplementary data.
[a] Stereocenters.
[b] R_n refer to Scheme 1.
[c] IC_{50}s (straight GSMs) and EC_{50}s (inverse GSMs) were determined as published previously.[3]

position. Therefore, the 4-position of the lower aromatic ring was chosen as an anchoring point for the diazirine moiety. Coupling of 4-(3-trifluoromethyl)-3*H*-diazirin-3-yl) benzaldehyde **14**, racemic amine **1** and 3-methyl-but-1-yne resulted in **AR80** as expected (Scheme 1 and Table 1). Given the modest potency gain of the enantiomeric pure forms of the modulators, the synthesis was carried out with racemic **1**, providing the racemic photoreactive compound **AR80** with preserved activity (**AR80** IC_{50} = 190 ± 14 nM (Aβ42); entry 11, Supplementary Figs. S1C and S2). Having successfully placed the photoreactive diazirine moiety, we next focused on the introduction of a biotin tag for affinity purification. Since the three-component coupling reaction proved tolerant to a large diversity of reactants, we attempted to introduce the biotin tag in the aliphatic side-chain of **AR262**. To

minimize perturbations induced by the bulky biotin tag, we selected a six-carbon-atoms long spacer for GSM **AR179** (IC_{50} = 1.0 ± 0 μM (Aβ42); entry 12, Supplementary Figs. S1D and S2). This analog was obtained by coupling silyl-protected amine **5**, 4-trifluoromethyl-benzaldehyde, and biotin-functionalized terminal alkyne **6**, followed by selective TBAF-mediated deprotection of the piperidine-bound carboxylic acid (Scheme 1 and Table 1). The introduction of the lipophilic diazirine moiety in **AR243** (IC_{50} = 500 ± 83 nM (Aβ42); entry 13) appeared to partially compensate the negative impact on potency of the biotin tag in **AR179**. We could therefore successfully obtain the complete photoreactive probe **AR243** (Scheme 1 and Table 1) with a purification tag, nanomolar activity, typical selectivity for an acidic GSM (Supplementary Figs. S1E and S2) and high scaffold similarity compared with the parent compound **GSM-1**. In an effort to further optimize the probe for experimentations in live cells, we aimed for the stabilization against cellular hydrolases of the side-chain supporting the biotin tag in **AR243**. Therefore, the ester bond was replaced by an amide bond in **AR367** using the N-Boc-protected terminal alkyne **9** in conjunction with racemic **1** and **14** in the A^3-coupling. HCl-treatment of the resulting coupling product released the free amine that was subsequently coupled to biotin, yielding the methylester **AR366** as a potent inverse photoprobe (EC_{50} = 1.1 ± 0.1 μM (Aβ42); entry 14, Supplementary Figs. S1F and S2). Saponification then gave the amide analog to **AR243**, named **AR367** (Scheme 1 and Table 1). Surprisingly, the amide modification induced a significant loss of activity (**AR367**: IC_{50} = 2.2 ± 0.1 μM (Aβ42); entry 15 and Supplementary Fig. S2), pointing to a high sensitivity to the polarity of the linker, as also previously reported for other photoreactive probes, also highlighting the advantage of tag-free strategies.[34,55] Noteworthy, the inverse activity of **AR366** underlines once more the disconnect between straight and inverse modulatory potencies as also noted previously for **AR499**. To eventually verify that the hydrolysis product of **AR243** does not contribute to the activity observed in cells, we synthesized the hydrolysis product **AR354** using the alkyne-acetate **7** followed by hydrolysis to obtain the free alcohol (Scheme 1 and Table 1). The low potency for **AR354** (IC_{50} = 2.0 ± 0.1 μM (Aβ42); entry 16 and Supplementary Fig. S2) confirmed the resilience of **AR243** towards ester hydrolysis and its suitability for labeling experiments in membrane preparations and in live cells.

2.2. Photolabeling

With the straight-GSM photoprobe **AR243** and the inverse probe **AR366** in hand, we performed the photolabeling experiments followed by purification on streptavidin beads, as described in a separate publication.[35] Briefly, we demonstrated that both the straight probe **AR243** and the inverse probe **AR366** bound in membrane preparations and in living cells to the N-terminal fragment of presenilin 1 (PS1), the catalytic subunit of the γ-secretase complex, in line with several independent studies.[34,38] For this, we treated N2a-ANPP cells that stably overexpress APP and all four subunits of the γ-secretase complex with 0.2 μM of the photo-probe **AR243** or DMSO vehicle and irradiated the live cells with 350 nm UV light. Subsequently, cellular membranes were prepared and proteins labeled with the photo-probe were affinity purified using streptavidin beads. The purified material was resolved on SDS gels and probed by Western blotting with antibodies against the four subunits of the γ-secretase complex or the substrate APP. Both probes selectively labeled the N-terminal Fragment of PS1, indicating that the effect of straight and inverse GSMs is mediated via direct binding to this γ-secretase subunit.[35]

3. Discussion

3.1. Synthesis and SAR

Here we report the design and synthesis of **GSM-1** derived diazirine-tagged γ-secretase modulators to elucidate their binding partner in a cell culture model. We developed an optimized protocol for the copper-(I)-catalyzed A^3-coupling, which was sufficiently mild to provide compatibility with heat sensitive diazirines. During the development of our frontrunner probe **AR243** we were able to obtain a small library of straight and inverse GSMs that facilitated the establishment of a preliminary structure–activity relationship. For straight GSMs we found that increased lipophilicity of the lower aromatic ring and the aliphatic side chain correlated well with increasing potency as expected for substances targeting membrane-embedded proteins. This is nicely illustrated by the disruptive effect of the polar biotin moiety on potency, partially reversed by introduction of the lipophilic diazirine moiety (see **AR179** (IC_{50} = 1.0 ± 0.0 μM) and **AR243** (500 ± 83 nM)). Additionally the presence of hydrogen-bond donors (Amide-NH: **AR367**; OH: **AR354**) in the linker region also led to a significant loss of potency (2.2 ± 0.1 μM and 2.0 ± 0.1 μM, respectively). Esterfication of the characteristic carboxylic acid moiety mediated the switch from straight to inverse modulation. Among the small subset of three inverse modulators, all showed comparable potencies on selectively raising Aß42 (Table 1; Entries 5, 7 and 13). Compared to the potencies of their respective straight GSMs (Table 1; Entries 1, 6 and 14) one might suggest a clear disconnect between the SAR of the inverse and straight GSMs. While the principles governing the switch between straight and inverse modulation are incompletely understood, shared binding sites are proposed based on photolabeling experiments, competition assays and the very high scaffold similarity.

3.2. Mode of action

The straight and inverse photoprobes **AR243** and **AR366**, respectively, allowed us to successfully carry out photolabeling experiments followed by biotin-affinity purification. Selective binding of both probes to the PS1-NTF was found, suggesting that both effects, straight and inverse modulation, are mediated via the same γ-secretase subunit.[35] This finding is in accordance with several independent studies and biochemical investigations.[22–24]

Indeed, two major compound classes have been identified to date, acidic and non-acidic imidazole based GSMs, raising questions about their respective targets.[19] We and others have reported cross-competition binding experiments between acidic and non-acidic GSMs, thereby providing insights into the binding sites for these molecules.[35,38] Competition between the photoreactive probe **AR243** and the acidic NSAID-like **JNJ-40418677** (Fig. 3) indicated a strong overlap in binding sites, as expected for homologous GSMs.[35] However, competitions experiments with non-acidic GSMs have provided more nuanced results, with a significant disconnect between competitiveness and chemical analogy. We observed a strong labeling competition between our acidic probe **AR243** and the imidazole-based non-acidic GSM compound **1** (Fig. 3), whereas structurally analogous and equally potent **E-2012** competed only partially. A similar disconnect has been independently reported in vice versa competition experiments with acidic GSMs against the non-acidic probe GSM photoprobe **RO-57-BpB**.[37] Therefore, it might be tempting to postulate distinct binding sites for acidic and non-acidic GSMs. However, conclusions based solely on these experiments should be avoided because of possible allosteric effects and artifacts linked to compound self-aggregation at the investigated concentration. Obviously, further

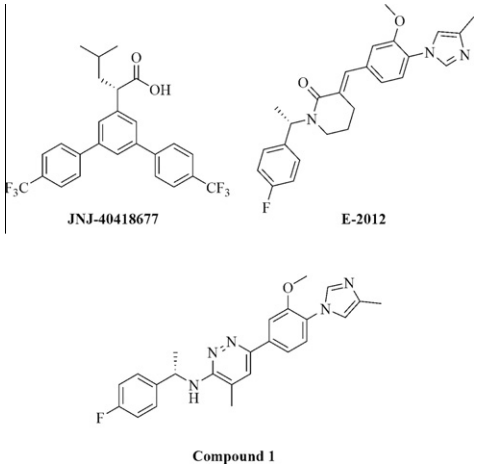

Figure 3. Compounds used for competition experiments. Compound 1, **E-2012**: Non-acidic GSMs. **JNJ-40418677**: Acidic GSM. Note the structural similarity between Compound **1** and **E-2012**.

studies using mass spectrometry-based proteomic analyses will be required to accurately map the respective binding sites.

In contrast, cross-competition experiments with GSMs and γ-secretase inhibitors (GSIs) strongly suggested distinct binding sites. Early cross-competition binding assays between a radiolabeled transition-state inhibitor and the GSM sulindac sulfide reported displacement in a non-competitive manner.[25] The finding was verified by a recent report showing unperturbed labeling of PS1-NTF by photoreactive acidic GSMs in competition with GSIs directed against the enzymatic active site, substrate-binding site or an allosteric site.[38] Moreover, this simultaneous binding of modulators and inhibitors allowed Li et al. to elegantly investigate the GSM-induced conformational changes in PS1 using photoreactive inhibitors directed towards several catalytic site subsites, demonstrating that GSMs allosterically modulate γ-secretase activity.[34] The proposed hydrophilic cavity in PS-1 around TMDs 6 and 7 forming the active site,[56–60] indeed lowers the probability to target this region with **GSM-1** analogs, due to the high lipophilicity of a scaffold with a *c*Log*P* of 7.92.

Despite the valuable information gained from photoaffinity labeling, the mode of action of GSMs remains obscure. Whereas the full inhibition of γ-secretase is well understood, the mode of action of modulators appears difficult to rationalize, and a high-resolution structure of the tetrameric γ-secretase complex is eagerly awaited.[58] The current model postulates a sequential cleavage of the C99 substrate each 3–4 amino acids starting at a ε–cleavage site near the cytoplasmic border, compatible with an alpha-helical conformation for the substrate.[61–65] Considering that the signature of GSMs comprises selective lowering of the pathogenic Aβ42 and increase of the shorter Aβ38 peptide, it is assumed that Aβ42 and Aβ38 might be interdependent, and that GSMs might promote a further cleavage step on Aβ42 to yield Aβ38 after a tetrapeptide release. However, a loose correlation in the Aβ40:Aβ38 ratio in cells expressing different FAD-associated PS1 mutants upon GSM treatment points to independent production lines for Aβ42 and Aβ38.[11,66] For instance, PS1-mutant cell lines, typically resistant to GSMs Aβ42 lowering effect, nevertheless appear sensitive to the Aβ38 elevating effect. Indeed, at least two separate product lines have been recently confirmed using high-resolution tandem mass spectrometry, a minor and pathogenic Aβ48-Aβ45-Aβ42 and a major Aβ49-Aβ46-Aβ43-Aβ40.[12,67] However, treatment with sulindac sulfide, a first generation GSM with low potency, did not allow establishing clearly the source of Aβ38.

Finally, the specificity of the initial ε−cleavage at the Aβ48 or Aβ49 positions might dictate the downstream outcome of the stepwise cleavages leading to Aβ42 or Aβ40 respectively, and a link between Aβ48 and Aβ42 has been reported in several PS1 mutants. Hence, it has been also proposed that the Aβ42 lowering effect of GSMs might be related to a shift in the initial ε−cleavage site.[68] However, recent experimental data show that the initial ε-cleavage site might not stay permanently upstream of Aβ42 and therefore might not be truly targeted by GSMs.[69,70] Altogether, photolabeling experiments with GSMs have provided extremely valuable information indicating direct binding to γ-secretase and an allosteric mode of action, which inspires further investigations to decipher the fascinating molecular mechanism of γ-secretase.

4. Conclusions

The photoreactive probe **AR243** is a novel γ−secretase modulator based on **GSM-1** with preserved potency. We also reported a preliminary structure–activity relationship pointing at preferential lipophilic substituents and relative tolerance to steric bulk. We could demonstrate that the biotin-tagged probe **AR243** bound in membrane preparation and in living cells to the N-terminal fragment of PS1 (the catalytic subunit of the γ-secretase complex). Moreover, we could obtain an inverse modulator **AR366** with micromolar potency, which labeled the same N-terminal fragment of PS1, providing an interesting tool for further investigations. Cross-competition experiments with other γ−secretase modulators point toward shared binding sites within PS1-NTF, which is in accordance to independent investigations by other groups.[34,35,37,38] However, while selective modulation of Aβ42 production is a promising strategy for drug development for Alzheimeŕs disease, further investigations are required to better understand the elusive link between GSM-induced PS1 conformational changes and the shifted proteolytic cleavage specificity of γ-secretase.

5. Experimental section

5.1. Chemistry

All reactions were performed under an inert atmosphere of argon or nitrogen, unless otherwise stated. ^{1}H NMR and ^{13}C NMR data were obtained on a Bruker Avance DPX 400 or DPX 500. Spectra were recorded at 298 K and the chemical shifts are expressed in ppm relative to solvent signals (^{1}H NMR: $CDCl_3$ 7.26; MeOD 3.31; DMSO-d_6 2.50; $CO(CD_3)_2$ 2.05; ^{13}C NMR: $CDCl_3$ 77.16; MeOD 49.00; DMSO-d_6 39.52; $CO(CD_3)_2$ 29.84). Compound purity was accessed by analytical HPLC (Shimadzu LC-10 HPLC-system; 4 × 150 mm M&N Nucleodur Isis 5 μm column) using a gradient system (t = 0–2 min: 80% H_2O + 0.1% TFA; 20% acetonitrile; ramp to 98% acetonitrile (t = 15 min; 6%/min); hold for 2 min; Injection at t = 1.5 min) and detection at 220 nm. Preparative HPLC was performed on a Shimadzu LC-8A system using different gradients (H_2O + 0.1% TFA and acetonitrile) at 5 ml/min on a 10 × 250 mm Supelco Ascentis C18 column. HRMS-spectra were recorded on a MAT 95 XL or MAT 90 mass spectrometer from Thermo Finnigan. Specific rotations were measured on a Autopol I from Rudolph Research Analytical (Hackettstown, NY, USA) in EtOH at stated concentrations. All reagents were obtained from Sigma–Aldrich (Munich, Germany), Alfa-Aesar (Karlsruhe, Germany), Acros Organics (Geel, Belgium), ABCR (Karlsruhe, Germany) or Fluorochem (Hadfield, UK) and were used as received.

5.1.1. General methods A and B for A^3-coupling

Method A (non-diazirine modulators): Inside a glovebox under N_2-atmosphere, a pressure tight vial was charged with aldehyde

(1 equiv), amine (2 equiv) and the respective terminal alkyne (2 equiv). CuBr (3 equiv) was added, followed by activated 4 Å molecular sieves (~1 g per 10 ml solvent). Toluene (7 ml/mmol aldehyde) was added and the reaction mixture heated to 90 °C under vigorous stirring for 24 h. The crude reaction mixture was filtered twice through Celite and a silica pad eluting with EtOAc (for biotin containing compounds 5% MeOH in DCM was used). After evaporation of the organic solvents, the crude extracts were purified by silica-gel chromatography or preparative HPLC as described below and in the Supplementary data. Method B (diazirine modulators): An equivalent setup as described above was used reducing the reaction temperature to 60 °C and prolonging the reaction time to 48 h.

5.1.2. Synthesis of diazirine-tagged benzaldehyde 14

5.1.2.1. Methyl 4-(2,2,2-trifluoroacetyl)benzoate 12. 4-(2,2,2-trifluoroacetyl)benzoic acid **11** (5 g, 22.92 mmol) was obtained according to Chen et al.,[51] dissolved in methanol (100 ml) and concd sulphuric acid (1.22 ml, 22.92 mmol) was added via syringe. The mixture was heated to 60 °C over night. It was neutralized with 1 M NaOH aq and concentrated. The obtained residue was partitioned between sat. $NaHCO_3$ aq and EtOAc. The organic layer was washed with brine, dried over $MgSO_4$ and evaporated to yield **12** as off-white solid that was used as obtained (5.20 g, 98%). Analytical data were in accordance to literature.[71]

^{1}H NMR (400 MHz, $(CD_3)_2CO$ δ = 3.96 (s, 3H), 8.21 (d, J = 8.5 Hz, 2H), 8.25 (d, J = 8.5 Hz, 2H).

^{13}C NMR (100 MHz, $(CD_3)_2CO$ δ = 53.04, 117.49 (q, J = 290.7 Hz), 130.92 (m), 130.94, 133.94, 137.04, 166.07, 180.82 (q, J = 35.2 Hz).

HRMS (EI; 70 eV) Calcd for $C_{10}H_7F_3O_3$ (M^+) 232.0347. Found 232.0348.

Purity (HPLC) = 95%; t_R = 12.54 min (Hydrate smears from 9.50 min to 12.54 min).

5.1.2.2. Methyl 4-(2,2,2-trifluoro-1-((tosyloxy)imino)ethyl)benzoate 13. Compound **12** (5.20 g, 22.40 mmol) and hydroxylamine hydrochloride (3.84 g, 56 mmol) were dissolved in a 1:2 mixture (37 ml) of methanol and pyridine and refluxed over night. Upon complete conversion the solvents were evaporated and the residue was partitioned between 5% HCl aq and DCM. After residual pyridine was washed out, the combined aqueous layers were extracted with DCM and organic layers were combined. It was washed with brine, dried over $MgSO_4$, filtered and evaporated. The residue was dissolved in DCM (40 ml) and triethylamine (7.75 ml, 56 mmol) was added. The mixture was cooled to 0 °C and tosylchloride (4.83 g, 25.3 mmol) was added in small portions over 10 min. The cooling bath was removed and the mixture was allowed to warm to rt during 2 h. It was poured onto 10% HCl aq and the layers were separated. The aqueous layer was washed with DCM, organic layers were combined, washed with brine, dried over $MgSO_4$, filtered and evaporated. The residue was purified on silica eluting with DCM to obtain **13** (isomeric mixture 2:3) as a white solid (8.63 g, 96%).

^{1}H NMR (400 MHz, $CDCl_3$) δ = (major isomer) 2.47 (s, 3H), 3.94 (s, 3H), 7.38 (m, 2H), 7.45 (d, J = 8.4 Hz), 7.87 (d, J = 8.1 Hz), 8.13 (d, J = 8.4 Hz).

^{13}C NMR (100 MHz, $CDCl_3$) δ = (major isomer) 21.88, 52.63, 119.5 (q, J = 277.5 Hz), 127.13, 128.58, 129.37, 129.90, 130.08, 131.07, 133.05, 146.50, 153.49 (q, J = 33.3 Hz), 165.87.

HRMS (ESI-TOF) Calcd for $C_{17}H_{14}F_3NO_5SNa$ (M+Na) 424.0442. Found 424.0440.

Purity (HPLC) = 98%; t_R = 15.41 min.

5.1.2.3. 4-(3-(Trifluoromethyl)-3*H*-diazirin-3-yl)benzaldehyde 14. Compound **13** (8.63 g, 21.50 mmol) was dissolved in DCM (11 ml) and transferred into a pressure tight vial. It was cooled to −78 °C and ammonia (~2 ml) was condensed into the solution. The vial was sealed and removed from the cooling after stirring for 30 min. While warming to rt stirring was continued over night. The excess ammonia was carefully evaporated and the formed precipitate filtered off. Evaporation of the filtrate gave the crude diaziridine that was dissolved in dry THF (60 ml) and cooled to 0 °C. A freshly prepared 0 °C solution of SDBBA (0.5 M in THF; 84 ml; 42 mmol) was added over 20 min and the mixture was stirred for another 20 min and then quenched by the slow addition of water (5 ml).[53] The solvent was evaporated and the oily residue partitioned between EtOAc and water. Layers were separated and the aqueous layer was washed several times with fresh portions of EtOAc. Combined organic layers are washed with brine, dried over $MgSO_4$ and evaporated to yield a yellowish oil that was directly used in the next step. To a −78 °C cold solution of oxalylchloride (3.58 ml, 41.7 mmol) in dry DCM (20 ml) a solution of dry DMSO (3.11 ml, 43.8 mmol) in dry DCM (20 ml) was slowly added over 20 min. The resulting solution was stirred for another 10 min and the crude from above was added over 20 min as a solution in dry DCM (40 ml). Stirring was continued for 15 min and the reaction was quenched by the slow addition of a solution of triethylamine (5.78 ml, 41.7 mmol) in dry DCM (10 ml). Upon complete addition the cooling was removed, allowing the reaction mixture to warm to rt and stirred for an additional hour.[52] Water was added and the layers formed are separated. The aqueous layer was washed with a fresh portion of DCM, organic layers were combined, washed with brine, dried, filtered and evaporated to obtain a yellow oil. Purification was performed on silica using pentane/Et_2O (9/1) and afforded **14** as a pale yellow liquid (1.824 g, 40%). Analytical data were in accordance to literature.[72]

^{1}H NMR (400 MHz, $CDCl_3$) δ = 7.35 (d, J = 8.4 Hz, 2H), 7.92 (d, J = 8.4 Hz, 2H), 10.04 (s, 1H).

^{13}C NMR (100 MHz, $CDCl_3$) δ = 28.61 (q, J = 40.6 Hz), 121.95 (q, J = 275.3 Hz), 127.13, 129.99, 135.40, 136.95.0, 191.20.

Purity (HPLC) = 98%; t_R = 13.66 min.

5.1.3. Synthesis of AR243

5.1.3.1. 2-(1-(7-((5-((3a*S*,4*S*,6a*R*)-2-Oxohexahydro-1*H*-thieno [3,4-d] imidazol-4-yl)pentanoyl)oxy)-1-(4-(3-(trifluoromethyl)-3*H*-diazirin-3-yl)phenyl)hept-2-yn-1-yl)-2-(4-(trifluoromethyl) phenyl)piperidin-4-yl)acetic acid AR243. About 110 mg of 4-(3-(trifluoromethyl)-3*H*-diazirin-3-yl)benzaldehyde **14** (0,52 mmol), 2-trimethylsilyl)ethyl 2-(2-(4-(trifluoromethyl)phenyl)piperidin-4-yl)acetate **5** (390 mg, 1.03 mmol), Hex-5-yn-1-yl 5-((3a*S*,4*S*,6a*R*)-2-oxohexahydro-1*H*-thieno [3,4-*d*]imidazol-4-yl)pentanoate **6** (335 mg, 1.03 mmol) and copper(I) bromide (222 mg, 1.55 mmol) were reacted in toluene (3.5 ml) according to general method B. The so obtained crude oil was dissolved in THF (15 ml) and TBAF (1 M in THF, 1.12 ml, 1.12 mmol) was slowly added at rt. The reaction was allowed to proceed for 2 h before dilution with EtOAc and water. The pH was set neutral and the final compound extracted with EtOAc. The organic layers were combined, washed with brine, dried over MgSO4, filtered and evaporated. The obtained crude oil was purified on preparative HPLC to afford **AR243** as a white foam (42 mg, 9.3%).

^{1}H NMR (400 MHz, MeOD) δ = 1.39–1.91 (m, 12H), 1.99 (m, 1H), 2.12 (m, 1H), 2.21 (m, 1H), 2.31 (d, J = 6.8 Hz, 2H), 2.36 (t, J = 7.4 Hz, 2H), 2.55 (td, J_1 = 6.8 Hz, J_2 = 2.1 Hz, 2H), 2.68 (d, J = 12.9 Hz, 1H), 2.89 (dd, J_1 = 12.9 Hz, J_2 = 4.9 Hz, 1H), 2.98 (m, 1H), 3.10–3.20 (m, 2H), 4.19 (t, J = 6.5 Hz), 4.28 (dd, J_1 = 8.1, J_2 = 4.5 Hz, 1H), 4.38–4.50 (m, 2H), 4.90 (s, 1H), 7.32 (d, J = 8.1 Hz, 2H), 7.61 (d, J = 8.1 Hz, 2H), 7.76–7.89 (m, 4H).

^{13}C NMR (100 MHz, MeOD) δ = 19.14, 25.98, 25.99, 29.17, 29.47, 29.71, 30.58, 33.31, 34.84, 40.30, 40.71, 41.02, 48.31, 56.97, 59.34, 61.62, 63.39, 65.03, 68.43, 71.58. 94.82, 123.45 (q, J = 275.2 Hz), 125.39 (q, J = 275.5 Hz), 127.64 (q, J = 3.3 Hz), 127.95, 129.92

(broad), 131.43, 131.59, 132.49 (q, J = 32.5 Hz), 136.60, 143.46, 166.09, 175.40, 175.52 (diazirine-carbon not resolved).

HRMS (ESI-TOF) for $C_{39}H_{43}F_6N_5O_5SH^+$ (M+H) 808.2967. Found 808.2938.

Purity (HPLC) = 97%; t_R = 13.87 min.

5.1.4. Synthesis of AR366

5.1.4.1. Methyl 2-(1-(7-(5-((3a*S*,4*S*,6a*R*)-2-oxohexahydro-1*H*-thieno[3,4-d]imidazol-4-yl)pentanamido)-1-(4-(3-(trifluoromethyl)-3*H*-diazirin-3-yl)phenyl)hept-2-yn-1-yl)-2-(4-(trifluoromethyl) phenyl) piperidin-4-yl)acetate AR366. Compound **14** (236 mg, 1.10 mmol), **1** (663 mg, 2.20 mmol), **9** (434 mg, 2.20 mmol) and copper(I) bromide (473 mg, 3.3 mmol) were reacted according to general method B. The crude oil was then treated with 4 M HCl in dioxane (1.38 ml, 5.5 mmol) for 2 h at rt. The solvent was removed in vacuo and the residue was dissolved in dry DMF (2.2 ml). DIPEA (575 µl, 3.3 mmol) was added, followed by biotin (403 mg, 1.65 mmol). The mixture was stirred for 5 min at rt and EDAC (422 mg, 2.2 mmol) was added. The reaction is left for 2 h and then diluted with EtOAc. Thorough extraction with water removed residual DMF; it was washed with brine, dried, filtered and evaporated. The resulting crude material was purified by prep. HPLC to afford **AR366** as off-white foam (226 mg, 25%).

^{1}H NMR (400 MHz, MeOD) δ = 1.34–1.47 (m, 3H), 1.52–1.77 (m, 10H), 1.82 (m, 1H), 1.92 (m, 1H), 2.16–2.26 (m, 4H), 2.35–2.47 (m, 4H), 2.66 (d, J = 12.9 Hz, 1H), 2.85 (dt, J_1 = 12.9, J_2 = 5.1 Hz, 1H), 3.14 (m, 1H), 3.26 (m, 2H), 3.61 (s, 3H), 3.67 (dd, J_1 = 11.3 Hz, J_2 = 8.3 Hz, 1H), 4.25 (dt, J_1 = 7.8 Hz, J_2 = 4.8 Hz, 1H), 4.39 (s, 1H), 4.44 (m, 1H), 7.18 (d, J = 8.1 Hz, 2H), 7.62 (d, J = 8 Hz, 2H), 7.64–7.70 (m, 4H).

^{13}C NMR (100 MHz, MeOD) δ = 19.06, 26.93, 27.54, 29.30. (q, J = 40.2 Hz), 29.47, 29.77, 29.92, 32.81, 34.91, 36.83, 39.84, 41.02, 41.56, 43.22, 47.00, 51.99, 56.97, 57.35, 61.58, 63.35, 66.72, 74.64, 90.75, 122.60 (q, J = 273.2 Hz), 125.67 (q, J = 271.1 Hz), 126.76 (q, J = 3.6 Hz), 127.28 129.02, 129.37 (broad), 129.84, 130.80 (q, J = 32.0 Hz), 143.01, 149.65, 166.04, 174.61, 175.96.

HRMS (ESI-TOF) Calcd for $C_{40}H_{46}F_6N_6O_4S$ (M+Na) 843.3103. Found 843.3069.

Purity (HPLC) = 98%; t_R = 13.19 min

Acknowledgments

We thank Karlheinz Baumann and Manfred Brockhaus (F. Hoffmann-La Roche Ltd, Switzerland) for carboxyl terminus-specific Aβ antibodies, Harrie Gijsen (Janssen Pharmaceutica NV, Belgium) for compounds 1 and JNJ-40418677, Sangram Sisodia (University of Chicago, USA) for N2a-ANPP cells, Hiroshi Mori (Osaka City University, Japan) for antibody PSN2, Edward Koo (UC San Diego, USA) for various reagents, and Herbert Waldmann (Max-Planck Institute of Molecular Physiology, Germany) and Guido Reifenberger (University of Duesseldorf, Germany) for encouragement and support.

This study was supported by the Competence Network Degenerative Dementias of the Federal Ministry of Education (Grant numbers 01 GI 1004D, 01 GI 1004C, 01 GI 1004B to C.P., B.B. and S.W.).

Supplementary data

Supplementary data associated with this article can be found, in the online version, at http://dx.doi.org/10.1016/j.bmc.2012.08.034. These data include MOL files and InChiKeys of the most important compounds described in this article.

References and notes

1. Puente, X. S.; Sanchez, L. M.; Overall, C. M.; Lopez-Otin, C. *Nat. Rev. Genet.* **2003**, *4*, 544.
2. Lopez-Otin, C.; Bond, J. S. *J. Biol. Chem.* **2008**, *283*, 30433.
3. Hahn, S.; Bruning, T.; Ness, J.; Czirr, E.; Baches, S.; Gijsen, H.; Korth, C.; Pietrzik, C. U.; Bulic, B.; Weggen, S. J. *Neurochemistry* **2011**, *116*, 385.
4. Kretner, B.; Fukumori, A.; Gutsmiedl, A.; Page, R. M.; Luebbers, T.; Galley, G.; Baumann, K.; Haass, C.; Steiner, H. *J. Biol. Chem.* **2011**, *286*, 15240.
5. Scheuner, D.; Eckman, C.; Jensen, M.; Song, X.; Citron, M.; Suzuki, N.; Bird, T. D.; Hardy, J.; Hutton, M.; Kukull, W.; Larson, E.; Levy-Lahad, E.; Viitanen, M.; Peskind, E.; Poorkaj, P.; Schellenberg, G.; Tanzi, R.; Wasco, W.; Lannfelt, L.; Selkoe, D.; Younkin, S. *Nat. Med.* **1996**, *2*, 864.
6. Thal, D. R.; Schultz, C.; Dehghani, F.; Yamaguchi, H.; Braak, H.; Braak, E. *Acta Neuropathol.* **2000**, *100*, 608.
7. Braak, H.; Braak, E.; Bohl, J.; Reintjes, R. *Neurosci. Lett.* **1996**, *210*, 87.
8. Bulic, B.; Pickhardt, M.; Mandelkow, E. M.; Mandelkow, E. *Neuropharmacology* **2010**, *59*, 276.
9. Guo, Q.; Wang, Z.; Li, H.; Wiese, M.; Zheng, H. *Cell Res.* **2012**, *22*, 78.
10. Zheng, H.; Koo, E. *Mol. Neurodegener.* **2011**, *6*, 27.
11. Czirr, E.; Cottrell, B. A.; Leuchtenberger, S.; Kukar, T.; Ladd, T. B.; Esselmann, H.; Paul, S.; Schubenel, R.; Torpey, J. W.; Pietrzik, C. U.; Golde, T. E.; Wiltfang, J.; Baumann, K.; Koo, E. H.; Weggen, S. *J. Biol. Chem.* **2008**, *283*, 17049.
12. Takami, M.; Nagashima, Y.; Sano, Y.; Ishihara, S.; Morishima-Kawashima, M.; Funamoto, S.; Ihara, Y. *J. Neurosci.* **2009**, *29*, 13042.
13. Wolfe, M. S. *Semin. Cell Dev. Biol.* **2009**, *20*, 219.
14. Bergmans, B. A.; De Strooper, B. *Lancet Neurol.* **2010**, *9*, 215.
15. Karran, E.; Mercken, M.; De Strooper, B. *Nat. Rev. Drug Discov.* **2011**, *10*, 698.
16. Hardy, J. *J. Neurochem.* **2009**, *110*, 1129.
17. Weggen, S.; Eriksen, J. L.; Das, P.; Sagi, S. A.; Wang, R.; Pietrzik, C. U.; Findlay, K. A.; Smith, T. E.; Murphy, M. P.; Bulter, T.; Kang, D. E.; Marquez-Sterling, N.; Golde, T. E.; Koo, E. H. *Nature* **2001**, *414*, 212.
18. Weggen, S.; Rogers, M.; Eriksen, J. *Trends Pharmacol. Sci.* **2007**, *28*, 536.
19. Bulic, B.; Ness, J.; Hahn, S.; Rennhack, A.; Jumpertz, T.; Weggen, S. *Curr. Neuropharmacol.* **2011**, *9*, 598.
20. Oehlrich, D.; Berthelot, D. J. C.; Gijsen, H. J. M. *J. Med. Chem.* **2011**, *54*, 669.
21. Wolfe, M. S. *J. Neurochem.* **2012**, *120*, 89.
22. Beher, D.; Clarke, E. E.; Wrigley, J. D.; Martin, A. C.; Nadin, A.; Churcher, I.; Shearman, M. S. *J. Biol. Chem.* **2004**, *279*, 43419.
23. Takahashi, Y.; Hayashi, I.; Tominari, Y.; Rikimaru, K.; Morohashi, Y.; Kan, T.; Natsugari, H.; Fukuyama, T.; Tomita, T.; Iwatsubo, T. *J. Biol. Chem.* **2003**, *278*, 18664.
24. Weggen, S.; Eriksen, J. L.; Sagi, S. A.; Pietrzik, C. U.; Ozols, V.; Fauq, A.; Golde, T. E.; Koo, E. H. *J. Biol. Chem.* **2003**, *278*, 31831.
25. Clarke, E. E.; Churcher, I.; Ellis, S.; Wrigley, J. D.; Lewis, H. D.; Harrison, T.; Shearman, M. S.; Beher, D. *J. Biol. Chem.* **2006**, *281*, 31279.
26. Lleo, A.; Berezovska, O.; Herl, L.; Raju, S.; Deng, A.; Bacskai, B. J.; Frosch, M. P.; Irizarry, M.; Hyman, B. T. *Nat. Med.* **2004**, *1065*, 10.
27. Uemura, K.; Lill, C. M.; Li, X.; Peters, J. A.; Ivanov, A.; Fan, Z.; Destrooper, B.; Bacskai, B. J.; Hyman, B. T.; Berezovska, O. *PLoS ONE* **2009**, *4*, e7893.
28. Kukar, T. L.; Ladd, T. B.; Bann, M. A.; Fraering, P. C.; Narlawar, R.; Maharvi, G. M.; Healy, B.; Chapman, R.; Welzel, A. T.; Price, R. W.; Moore, B.; Rangachari, V.; Cusack, B.; Eriksen, J.; Jansen-West, K.; Verbeeck, C.; Yager, D.; Eckman, C.; Ye, W.; Sagi, S.; Cottrell, B. A.; Torpey, J.; Rosenberry, T. L.; Fauq, A.; Wolfe, M. S.; Schmidt, B.; Walsh, D. M.; Koo, E. H.; Golde, T. E. *Nature* **2008**, *453*, 925.
29. Richter, L.; Munter, L. M.; Ness, J.; Hildebrand, P. W.; Dasari, M.; Unterreitmeier, S.; Bulic, B.; Beyermann, M.; Gust, R.; Reif, B.; Weggen, S.; Langosch, D.; Multhaup, G. *Proc. Natl. Acad. Sci. U.S.A.* **2010**, *107*, 14597.
30. Botev, A.; Munter, L. M.; Wenzel, R.; Richter, L.; Althoff, V.; Ismer, J.; Gerling, U.; Weise, C.; Koksch, B.; Hildebrand, P. W.; Bittl, R.; Multhaup, G. *Biochemistry* **2011**, *50*, 828.
31. Beel, A. J.; Barrett, P.; Schnier, P. D.; Hitchcock, S. A.; Bagal, D.; Sanders, C. R.; Jordan, J. B. *Biochemistry* **2009**, *48*, 11837.
32. Barrett, P. J.; Sanders, C. R.; Kaufman, S. A.; Michelsen, K.; Jordan, J. B. *Biochemistry* **2011**, *50*, 10328.
33. Leach, A. R.; Hann, M. M. *Curr. Opin. Chem. Biol.* **2011**, *15*, 489.
34. Crump, C. J.; Fish, B. A.; Castro, S. V.; Chau, D. M.; Gertsik, N.; Ahn, K.; Stiff, C.; Pozdnyakov, N.; Bales, K. R.; Johnson, D. S.; Li, Y. M. *ACS Chem. Neurosci.* **2011**, *2*, 705.
35. Jumpertz, T.; Rennhack, A.; Ness, J.; Baches, S.; Pietrzik, C. U.; Bulic, B.; Weggen, S. *PLoS ONE* **2012**, *7*, e30484.
36. Kounnas, M. Z.; Danks, A. M.; Cheng, S.; Tyree, C.; Ackerman, E.; Zhang, X.; Ahn, K.; Nguyen, P.; Comer, D.; Mao, L.; Yu, C.; Pleynet, D.; Digregorio, P. J.; Velicelebi, G.; Stauderman, K. A.; Comer, W. T.; Mobley, W. C.; Li, Y. M.; Sisodia, S. S.; Tanzi, R. E.; Wagner, S. L. *Neuron* **2010**, *67*, 769.
37. Ebke, A.; Luebbers, T.; Fukumori, A.; Shirotani, K.; Haass, C.; Baumann, K.; Steiner, H. *J. Biol. Chem.* **2011**, *286*, 37181.
38. Ohki, Y.; Higo, T.; Uemura, K.; Shimada, N.; Osawa, S.; Berezovska, O.; Yokoshima, S.; Fukuyama, T.; Tomita, T.; Iwatsubo, T. *EMBO J.* **2011**, *30*, 4815.
39. Dubinsky, L.; Krom, B. P.; Meijler, M. M. *Bioorg. Med. Chem.* **2012**, *20*, 554.
40. Blencowe, A.; Hayes, W. *Soft Matter* **2005**, *1*, 178.
41. Kotzyba-Hibert, F.; Kapfer, I.; Goeldner, M. *Angew. Chem., Int. Ed.* **1995**, *34*, 1296.
42. Fleming, S. A. *Tetrahedron* **1995**, *51*, 12479.
43. Brunner, J.; Senn, H.; Richards, F. M. *J. Biol. Chem.* **1980**, *255*, 3313.
44. Hannam, J. C.; Kulagowski, J. J.; Madin, A.; Ridgill, M. P.; Seward, E. M. WO/2006/043064 2006.
45. Gommermann, N.; Koradin, C.; Polborn, K.; Knochel, P. *Angew. Chem., Int. Ed.* **2003**, *42*, 5763.
46. Li, P.; Zhang, Y.; Wang, L. *Chem. Eur. J.* **2009**, *15*, 2045.

47. Zhang, Y.; Li, P.; Wang, M.; Wang, L. *J. Org. Chem.* **2009**, *74*, 4364.
48. Wei, C.; Li, C.-J. *J. Am. Chem. Soc.* **2003**, *125*, 9584.
49. Sharma, S.; Oehlschlager, A. C. *J. Org. Chem.* **1989**, *54*, 5064.
50. Fischer, C.; Munoz, B.; Rivkin, A. A. WO/2008/097538 2008.
51. Chen, L. S.; Chen, G. J.; Tamborski, C. *J. Organomet. Chem.* **1983**, *251*, 139.
52. Richardson, S. K.; Ife, R. J. *J. Chem. Soc., Perkin Trans. 1* **1989**, 1172.
53. Song, J. I.; An, D. K. *Chem. Lett.* **2007**, *36*, 886.
54. Narlawar, R.; Baumann, K.; Czech, C.; Schmidt, B. *Bioorg. Med. Chem. Lett.* **2007**, *17*, 5428.
55. Kan, T.; Kita, Y.; Morohashi, Y.; Tominari, Y.; Hosoda, S.; Tomita, T.; Natsugari, H.; Iwatsubo, T.; Fukuyama, T. *Org. Lett.* **2007**, *9*, 2055.
56. Sato, C.; Morohashi, Y.; Tomita, T.; Iwatsubo, T. *J. Neurosci.* **2006**, *26*, 12081.
57. Tolia, A.; Chavez-Gutierrez, L.; De Strooper, B. *J. Biol. Chem.* **2006**, *281*, 27633.
58. Osenkowski, P.; Li, H.; Ye, W.; Li, D.; Aeschbach, L.; Fraering, P. C.; Wolfe, M. S.; Selkoe, D. J. *J. Mol. Biol.* **2009**, *385*, 642.
59. Takagi, S.; Tominaga, A.; Sato, C.; Tomita, T.; Iwatsubo, T. *J. Neurosci.* **2010**, *30*, 15943.
60. Sobhanifar, S.; Schneider, B.; Löhr, F.; Gottstein, D.; Ikeya, T.; Mlynarczyk, K.; Pulawski, W.; Ghoshdastider, U.; Kolinski, M.; Filipek, S.; Güntert, P.; Bernhard, F.; Dötsch, V. *Proc. Natl. Acad. Sci. U.S.A.* **2010**, *107*, 9644.
61. Sastre, M.; Steiner, H.; Fuchs, K.; Capell, A.; Multhaup, G.; Condron, M. M.; Teplow, D. B.; Haass, C. *EMBO Rep.* **2001**, *2*, 835.
62. Yu, C.; Kim, S. H.; Ikeuchi, T.; Xu, H.; Gasparini, L.; Wang, R.; Sisodia, S. S. *J. Biol. Chem.* **2001**, *276*, 43756.
63. Weidemann, A.; Eggert, S.; Reinhard, F. B.; Vogel, M.; Paliga, K.; Baier, G.; Masters, C. L.; Beyreuther, K.; Evin, G. *Biochemistry* **2002**, *41*, 2825.
64. Lichtenthaler, S. F.; Beher, D.; Grimm, H. S.; Wang, R.; Shearman, M. S.; Masters, C. L.; Beyreuther, K. *Proc. Natl. Acad. Sci. U.S.A.* **2002**, *99*, 1365.
65. Gu, Y.; Misonou, H.; Sato, T.; Dohmae, N.; Takio, K.; Ihara, Y. *J. Biol. Chem.* **2001**, *276*, 35235.
66. Page, R. M.; Baumann, K.; Tomioka, M.; Perez-Revuelta, B. I.; Fukumori, A.; Jacobsen, H.; Flohr, A.; Luebbers, T.; Ozmen, L.; Steiner, H.; Haass, C. *J. Biol. Chem.* **2008**, *283*, 677.
67. Qi-Takahara, Y.; Morishima-Kawashima, M.; Tanimura, Y.; Dolios, G.; Hirotani, N.; Horikoshi, Y.; Kametani, F.; Maeda, M.; Saido, T. C.; Wang, R.; Ihara, Y. *J. Neurosci.* **2005**, *25*, 436.
68. Kakuda, N.; Funamoto, S.; Yagishita, S.; Takami, M.; Osawa, S.; Dohmae, N.; Ihara, Y. *J. Biol. Chem.* **2006**.
69. Mori, K.; Okochi, M.; Tagami, S.; Nakayama, T.; Yanagida, K.; Kodama, T. S.; Tatsumi, S.-i.; Fujii, K.; Tanimukai, H.; Hashimoto, R.; Morihara, T.; Tanaka, T.; Kudo, T.; Funamoto, S.; Ihara, Y.; Takeda, M. *Psychogeriatrics* **2010**, *10*, 117.
70. Chavez-Gutierrez, L.; Bammens, L.; Benilova, I.; Vandersteen, A.; Benurwar, M.; Borgers, M.; Lismont, S.; Zhou, L.; Van Cleynenbreugel, S.; Esselmann, H.; Wiltfang, J.; Serneels, L.; Karran, E.; Gijsen, H.; Schymkowitz, J.; Rousseau, F.; Broersen, K.; De Strooper, B. *EMBO J.* **2012**, *31*, 2261.
71. Uno, H.; Nibu, N.; Misobe, N. *Bull. Chem. Soc. Jpn.* **1999**, *72*, 1365.
72. Kwiatkowski, S.; Crocker, P. J.; Chavan, A. J.; Nobuyuki, I.; Haley, B. E.; Watt, D. S.; Ren-jye, H. *Tetrahedron Lett.* **1990**, *31*, 2093.